

## Femtosecond laser-induced nanostructure formation in Sb<sub>2</sub>Te<sub>3</sub>

Yuwei Li, Vladimir A. Stoica, Lynn Endicott, Guoyu Wang, Huarui Sun et al.

Citation: *Appl. Phys. Lett.* **99**, 121903 (2011); doi: 10.1063/1.3634014

View online: <http://dx.doi.org/10.1063/1.3634014>

View Table of Contents: <http://apl.aip.org/resource/1/APPLAB/v99/i12>

Published by the [AIP Publishing LLC](#).

---

### Additional information on *Appl. Phys. Lett.*

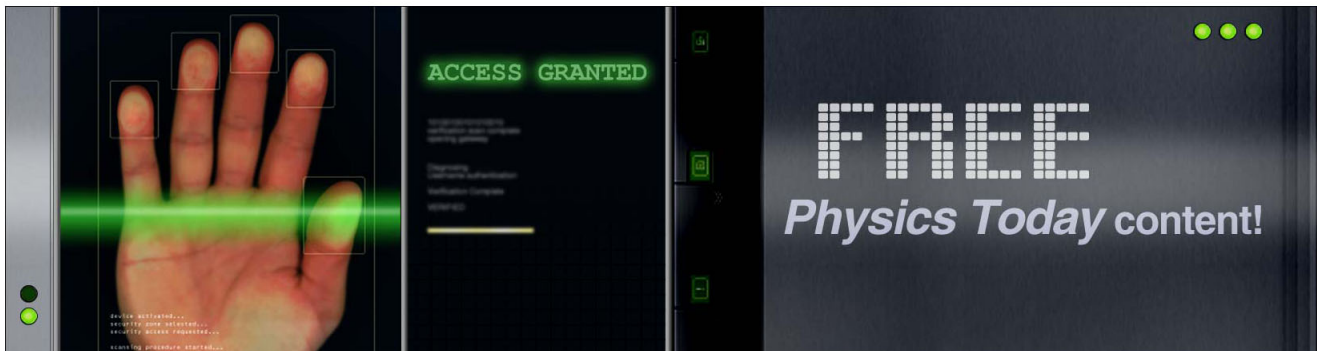
Journal Homepage: <http://apl.aip.org/>

Journal Information: [http://apl.aip.org/about/about\\_the\\_journal](http://apl.aip.org/about/about_the_journal)

Top downloads: [http://apl.aip.org/features/most\\_downloaded](http://apl.aip.org/features/most_downloaded)

Information for Authors: <http://apl.aip.org/authors>

## ADVERTISEMENT



# Femtosecond laser-induced nanostructure formation in $\text{Sb}_2\text{Te}_3$

Yuwei Li,<sup>1,2</sup> Vladimir A. Stoica,<sup>1,2</sup> Lynn Endicott,<sup>1</sup> Guoyu Wang,<sup>1,2</sup> Huarui Sun,<sup>2,3</sup>  
Kevin P. Pipe,<sup>2,3</sup> Ctirad Uher,<sup>1,2,4</sup> and Roy Clarke<sup>1,2,4,a)</sup>

<sup>1</sup>Department of Physics, University of Michigan, Ann Arbor, Michigan 48109, USA

<sup>2</sup>Center for Solar and Thermal Energy Conversion, University of Michigan, Ann Arbor, Michigan 48109, USA

<sup>3</sup>Department of Mechanical Engineering, University of Michigan, Ann Arbor, Michigan 48109, USA

<sup>4</sup>Applied Physics Program, University of Michigan, Ann Arbor, Michigan 48109, USA

(Received 20 April 2011; accepted 5 August 2011; published online 19 September 2011)

We report femtosecond laser-induced nanotracks in highly absorbing  $\text{Sb}_2\text{Te}_3$ . Groups of nanotracks are observed with widths  $\sim 50$  nm and periodicity  $\sim 130$  nm, their area of coverage extending with the increase of laser fluence. We demonstrate that under a narrow range of laser fluences and laser irradiation times, long highly aligned nanotracks can be formed in  $\text{Sb}_2\text{Te}_3$ . The results suggest a promising avenue for laser nanostructuring of chalcogenide thermoelectrics, with implications for high efficiency thermoelectric energy conversion. © 2011 American Institute of Physics. [doi:10.1063/1.3634014]

Antimony telluride ( $\text{Sb}_2\text{Te}_3$ ) is one of the most widely used materials for thermoelectric applications.<sup>1</sup> Presently, it is of interest to study the thermoelectric properties of low dimensional structures such as thin films, wires, and quantum dots. These structures have been predicted<sup>2,3</sup> to have significantly higher energy conversion efficiency than bulk forms of the material on account of energy filtering, quantum confinement, and enhanced phonon scattering on multiple boundaries. Recent measurements on  $\text{Sb}_2\text{Te}_3$  nanowires suggest that thermoelectric power enhancement may be possible at the smallest wire diameters.<sup>4</sup> In addition to its attractive thermoelectric properties, the band structure of  $\text{Sb}_2\text{Te}_3$  makes it a promising candidate material for realization of a topological insulator,<sup>5</sup> which is characterized by conductive states at the surface and insulating states in the bulk. Of particular interest are one-dimensional nanostructures that provide a means to tune the surface-to-volume ratio and thereby enhance the contribution of exotic surface states.<sup>6</sup> Therefore, the preparation of nanostructures in  $\text{Sb}_2\text{Te}_3$  has wide potential applications.

Among the various efforts to prepare nanostructures, femtosecond laser-induced modification has attracted considerable interest.<sup>7–16</sup> In particular, structures with periods significantly smaller than the laser wavelength are observed predominantly in transparent and semi-transparent materials,<sup>10–16</sup> for which the imaginary part  $\kappa$  of the complex refractive index  $\tilde{n} = n + i\kappa$  is negligible. For example, a well studied transparent material is diamond,<sup>17–20</sup> in which recent efforts have clearly demonstrated highly aligned and highly uniform nanostructures written with a femtosecond laser approach.<sup>20</sup> On the other hand, similar observations are rarely reported for absorptive materials with  $\kappa$  comparable to  $n$ . As a result, femtosecond laser-induced nanostructure formation has remained elusive for certain technologically important materials such as  $\text{Sb}_2\text{Te}_3$ , a narrow bandgap semiconductor which is highly absorbing in the visible and near-infrared spectral regions.<sup>21</sup>

In this letter, we report on the formation of femtosecond laser-induced nanotracks on both bulk and epitaxial thin film forms of  $\text{Sb}_2\text{Te}_3$ . The nanotracks have widths  $\sim 50$  nm and periods  $\Lambda \sim 130$  nm, less than 10% of the laser wavelength,  $\lambda$ . Our results describing the dependence of  $\text{Sb}_2\text{Te}_3$  material modification on both the laser fluence and irradiation time highlight the formation of such nanostructures in strongly absorbing material.

The experiments were performed on a bulk  $\text{Sb}_2\text{Te}_3$  sample and several  $\text{Sb}_2\text{Te}_3$  thin films grown on  $\text{Al}_2\text{O}_3$  (sapphire) substrates by molecular beam epitaxy (MBE). A fiber laser provided 100 femtosecond pulses at a repetition rate of 100 MHz, with a wavelength of 1580 nm. The linearly polarized laser pulses were focused at normal incidence onto the surface of the film with a focal spot diameter of  $\sim 3$   $\mu\text{m}$ . The laser fluence incident on the film surface could be varied from approximately 3  $\text{mJ}/\text{cm}^2$  to 6  $\text{mJ}/\text{cm}^2$  by using a half-wave plate followed by a polarizer. The samples were mounted on an xyz-translation stage that was scanned at different speeds from 1  $\mu\text{m}/\text{s}$  to 500  $\mu\text{m}/\text{s}$  in the direction perpendicular to the laser propagation. This allowed the laser to scan across the sample as it irradiated the surface. The laser-writing process was carried out under ambient conditions. The laser-scanned regions were then examined by scanning electron microscopy (SEM) and atomic force microscopy (AFM).

Figure 1 shows an SEM image of laser-induced nanostructure formation on a 200 nm  $\text{Sb}_2\text{Te}_3$  film. The surface roughness of the film, defined as the arithmetical average of the surface profile,  $R_a$ , is  $\sim 5$  nm. The irradiation fluence and scan speed were 6.3  $\text{mJ}/\text{cm}^2$  and 10  $\mu\text{m}/\text{s}$ , respectively. Four highly aligned nanotracks are clearly visible in the irradiated region, with widths in the range of 45–80 nm and an average spacing,  $\Lambda$ , of  $130 \pm 10$  nm. The observed spacing is consistent with an estimate based on the lateral interference condition<sup>16</sup>  $\Lambda = \lambda/2n = 131.7$  nm ( $\lambda = 1580$  nm and  $n \approx 6$ ).<sup>21</sup> AFM measurements reveal that the peak-to-valley amplitude of the nanotracks is approximately 50 nm, which is close to the laser's penetration depth in  $\text{Sb}_2\text{Te}_3$  ( $\delta = \lambda/4\pi\kappa \approx 60$  nm). Also, on bulk  $\text{Sb}_2\text{Te}_3$ , we observed more than ten highly aligned tracks with widths of approximately 40 nm and lengths of at least 19  $\mu\text{m}$ . This is a clear indication that we

<sup>a)</sup> Author to whom correspondence should be addressed. Electronic mail: royce@umich.edu.

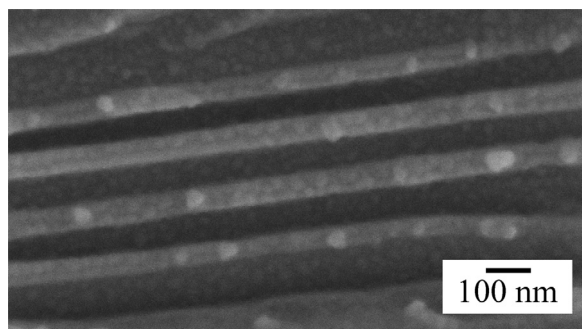


FIG. 1. SEM image of nanotracks on a 200 nm  $\text{Sb}_2\text{Te}_3$  film after irradiation by a 1580 nm femtosecond laser with a fluence of  $6.3 \text{ mJ/cm}^2$  and a scan speed of  $10 \mu\text{m/s}$ .

film surface, while near the antinodes of the interference pattern, the high laser intensity leads to periodic removal of material from the surface of the film. As the laser fluence grows from  $3.9 \text{ mJ/cm}^2$  to  $6.3 \text{ mJ/cm}^2$ , the amplitude of the interference standing wave increases, thereby expanding the areas around the antinodes in which the laser intensity exceeds the threshold for material removal. Consequently, the nanostructure formation extends outwards into the annealed areas as the laser fluence increases (see Fig. 2).

The nanostructure morphology depends not only on laser fluence but also on the laser irradiation time, which is controlled by the scan speed. Fig. 3 shows two regions on the same film as in Fig. 1 irradiated by a laser fluence of  $6.3 \text{ mJ/cm}^2$  at two different scan speeds:  $1 \mu\text{m/s}$  and  $10 \mu\text{m/s}$ . At  $1 \mu\text{m/s}$ , the irradiated region is dominated by quasi-ordered nanostructures. As the speed increases to  $10 \mu\text{m/s}$  and the corresponding irradiation time decreases by a factor of 10, the irradiated region becomes covered with highly ordered and continuous nanotracks with spacing comparable to their width.

The substantial change in nanotrack morphology with laser irradiation time may be related to the complex interaction processes between the ultrafast laser and the film, which include not only thermal mechanisms but also electronic effects.<sup>24</sup> We suggest that for the slower speed (longer irradiation time) of  $1 \mu\text{m/s}$ , the large amount of accumulated heat<sup>25</sup> melts the surface of  $\text{Sb}_2\text{Te}_3$ , and the quasi-ordered nanostructures of Fig. 3(a) originate from a liquid state. For the faster speed of  $10 \mu\text{m/s}$  (shorter irradiation time), the surface of  $\text{Sb}_2\text{Te}_3$  is not hot enough to melt, and the nanotrack formation results from the modification of a solid phase. In addition, results from energy dispersive x-ray spectroscopy show that the laser-modified regions in Fig. 3(b) retain the  $\text{Sb}_2\text{Te}_3$  stoichiometry. Optical phonon spectroscopy also indicates that  $\text{Sb}_2\text{Te}_3$  decomposition observed previously<sup>26</sup> is insignificant at such high scan speeds and short irradiation times. This is a promising result for the fabrication of stoichiometric  $\text{Sb}_2\text{Te}_3$  nanowires.

are able to form nanotracks on both bulk and thin film forms of  $\text{Sb}_2\text{Te}_3$ .

In order to study the dependence of nanostructure formation and morphology on laser fluence, we irradiated three regions at a speed of  $10 \mu\text{m/s}$  on another 200 nm  $\text{Sb}_2\text{Te}_3$  film with roughness  $R_a \sim 23 \text{ nm}$ , each with a different fluence:  $3.9 \text{ mJ/cm}^2$ ,  $5.2 \text{ mJ/cm}^2$ , and  $6.3 \text{ mJ/cm}^2$  (Fig. 2). For all three regions, groups of nanotracks were observed to develop with a  $1.5 \pm 0.1 \mu\text{m}$  periodicity matching that of the laser wavelength. These nanotrack groups were separated by smoother regions which appear to be annealed. As the fluence increased, the areas covered by the nanotracks expanded into the annealed regions and eventually covered the entire irradiated area; however, over the range of fluences tested, we observed no change in the period of the nanotracks themselves ( $\sim 130 \text{ nm}$ ). Furthermore, the fluence threshold for nanotrack formation in this sample appears to be smaller than that of the smoother sample shown in Fig. 1.

We analyze the periodic appearance of nanotrack groups and its dependence on laser fluence in terms of the following processes: the interference between the normal-incidence laser beam and the surface-scattered electromagnetic wave creates a periodic variation of laser intensity along the sample's surface with a period equal to the laser's wavelength.<sup>22,23</sup> Near the nodes of the interference pattern, the low intensity laser irradiation causes mild annealing of the

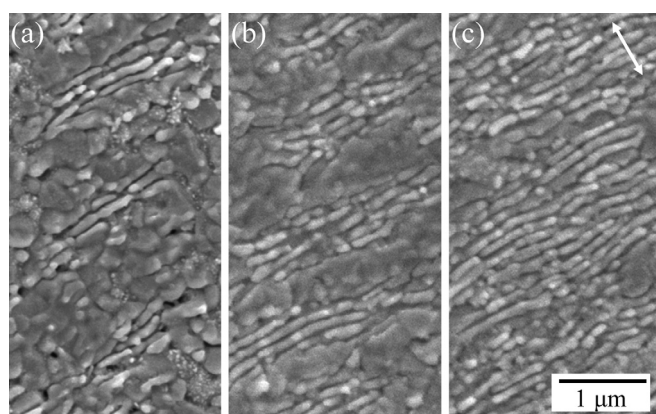


FIG. 2. SEM images of nanotracks on a 200 nm  $\text{Sb}_2\text{Te}_3$  film after irradiation by a 1580 nm femtosecond laser with a scan speed of  $10 \mu\text{m/s}$  and fluences of (a)  $3.9 \text{ mJ/cm}^2$ , (b)  $5.2 \text{ mJ/cm}^2$ , and (c)  $6.3 \text{ mJ/cm}^2$ . The arrow indicates the plane of laser polarization. Note that as the laser fluence increases, the areas covered by nanotracks extend into the annealed areas.

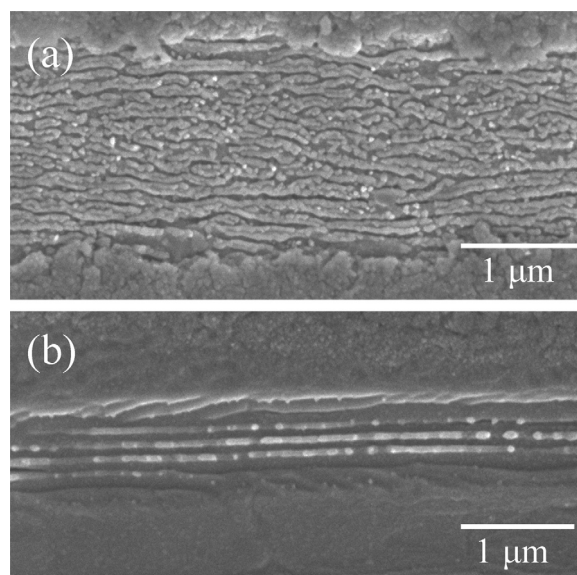


FIG. 3. SEM images of nanotracks on a 200 nm  $\text{Sb}_2\text{Te}_3$  film after irradiation by a 1580 nm femtosecond laser with a fluence of  $6.3 \text{ mJ/cm}^2$  and scan speeds of (a)  $1 \mu\text{m/s}$  and (b)  $10 \mu\text{m/s}$ .



157 The studies of laser-induced nanostructures presented  
 158 here have important implications for controlling the physical  
 159 properties of  $\text{Sb}_2\text{Te}_3$ . In particular, one would expect significant  
 160 changes in thermal and electronic transport to arise  
 161 from the formation of nanostructures. Indeed, using time-  
 162 domain thermoreflectance techniques<sup>27</sup> we have measured  
 163 reductions in the thermal conductivity of laser-modified  
 164 regions of  $\text{Sb}_2\text{Te}_3$  thin films compared to unmodified  
 165 regions. These results, which are the subject of ongoing  
 166 investigations to be reported in a separate publication, dem-  
 167 onstrate one example of the potential benefits of femtosec-  
 168 ond laser-induced nanostructuring for improving a material's  
 169 thermoelectric efficiency.

170 In conclusion, we have observed femtosecond laser-  
 171 induced nanostructures in  $\text{Sb}_2\text{Te}_3$  in the strongly absorbing  
 172 regime. This observation highlights the encouraging possibil-  
 173 ity of their formation not only in transparent dielectrics but  
 174 also in strongly absorbing narrow-gap materials that are im-  
 175 portant to future technologies. Most importantly, our meas-  
 176 urements have revealed the existence of a regime in which  
 177 ordered nanotracks emerge under ultrafast laser irradiation,  
 178 not simply as a result of melting and recrystallization. Finally,  
 179 we note that similar nanostructure formation has been  
 180 observed in other absorptive layered materials typified by van  
 181 der Waals bonding.<sup>18</sup> It is an interesting open question what  
 182 role the weakly bonded layers in  $\text{Sb}_2\text{Te}_3$  play during laser  
 183 modification. Our work serves as an important step toward  
 184 controlled formation of nanostructures in  $\text{Sb}_2\text{Te}_3$ . We expect  
 185 that similar laser-induced nanostructure formation may also  
 186 occur in other tetradymite-type materials, which form a major  
 187 branch of current thermoelectric technology.

188 This material is based on work supported as part of the  
 189 Center for Solar and Thermal Energy Conversion, an Energy  
 190 Frontier Research Center funded by the U.S. Department of  
 191 Energy, Office of Science, Office of Basic Energy Sciences  
 192 under Award No. DE-SC00000957. The authors would also  
 193 like to thank the University of Michigan Electron  
 194 Microbeam Analysis Laboratory for providing access to  
 195 microscopy facilities.

196

- <sup>1</sup>G. J. Snyder and E. S. Toberer, *Nature Mater.* **7**, 105 (2008). 197
- <sup>2</sup>L. D. Hicks and M. S. Dresselhaus, *Phys. Rev. B* **47**, 12727 (1993). 198
- <sup>3</sup>L. D. Hicks and M. S. Dresselhaus, *Phys. Rev. B* **47**, 16631 (1993). 199
- <sup>4</sup>Y. M. Zuev, J. S. Lee, C. Galloy, H. Park, and P. Kim, *Nano Lett.* **10**, 200 201
- <sup>5</sup>H. Zhang, C. Liu, X. Qi, X. Dai, Z. Fang, and S. Zhang, *Nat. Phys.* **5**, 438 202
- <sup>6</sup>D. Kong, J. C. Randel, H. Peng, J. J. Cha, S. Meister, K. Lai, Y. Chen, 203
- Z. Shen, H. C. Manoharan, and Y. Cui, *Nano Lett.* **10**, 329 (2010). 204
- <sup>7</sup>J. Bonse, A. Rosenfeld, and J. Krüger, *J. Appl. Phys.* **106**, 104910 (2009). 205
- <sup>8</sup>M. Huang, F. Zhao, Y. Cheng, N. Xu, and Z. Xu, *ACS Nano* **3**, 4062 206
- (2009). 207
- <sup>9</sup>J. Bonse and J. Krüger, *J. Appl. Phys.* **108**, 034903 (2010). 208
- <sup>10</sup>A. Borowiec and H. K. Haugen, *Appl. Phys. Lett.* **82**, 4462 (2003). 209
- <sup>11</sup>Y. Shimotsuma, P. G. Kazansky, J. Qiu, and K. Hirao, *Phys. Rev. Lett.* **91**, 210
- 247405 (2003). 211
- <sup>12</sup>N. Yasumaru, K. Miyazaki, and J. Kiuchi, *Appl. Phys. A* **81**, 933 (2005). 212
- <sup>13</sup>T. Q. Jia, H. X. Chen, M. Huang, F. L. Zhao, J. R. Qiu, R. X. Li, Z. Z. Xu, 213
- X. K. He, J. Zhang, and H. Kuroda, *Phys. Rev. B* **72**, 125429 (2005). 214
- <sup>14</sup>M. Shen, J. E. Carey, C. H. Crouch, M. Kandyla, H. A. Stone, and 215
- E. Mazur, *Nano Lett.* **8**, 2087 (2008). 216
- <sup>15</sup>C. Wang, H. Huo, M. Johnson, M. Shen, and E. Mazur, *Nanotechnology* 217
- 21**, 075304 (2010). 218
- <sup>16</sup>R. Buividas, L. Rosa, R. Sliupas, T. Kudrius, G. Slekyas, V. Datsyuk, and 219
- S. Juodkazis, *Nanotechnology* **22**, 055304 (2011). 220
- <sup>17</sup>Q. Wu, Y. Ma, R. Fang, Y. Liao, Q. Yu, X. Chen, and K. Wang, *Appl.* 221
- Phys. Lett.* **82** 1703 (2003). 222
- <sup>18</sup>M. Huang, F. Zhao, Y. Cheng, N. Xu, and Z. Xu, *Phys. Rev. B* **79**, 125436 223
- (2009). 224
- <sup>19</sup>E. M. Hsu, N. A. Mailman, G. A. Botton, and H. K. Haugen, *Appl. Phys.* 225
- A* **103**, 185 (2011). 226
- <sup>20</sup>M. Shinoda, R. R. Gattass, and E. Mazur, *J. Appl. Phys.* **105**, 053102 227
- (2009). 228
- <sup>21</sup>W. Richter, A. Krost, U. Nowak, and E. Anastassakis, *Z. Phys. B: Con-* 229
- dens. Matter* **49**, 191 (1982). 230
- <sup>22</sup>J. E. Sipe, J. F. Young, J. S. Preston, and H. M. van Driel, *Phys. Rev. B* 231
- 27**, 1141 (1983). 232
- <sup>23</sup>J. F. Young, J. S. Preston, H. M. van Driel, and J. E. Sipe, *Phys. Rev. B* 233
- 27**, 1155 (1983). 234
- <sup>24</sup>X. Liu, D. Du, and G. Mourou, *IEEE J. Quantum Electron.* **33**, 1706 235
- (1997). 236
- <sup>25</sup>The large heat accumulation is associated with the high repetition rate of 237
- our laser (100 MHz), along with the poor thermal conductivity of  $\text{Sb}_2\text{Te}_3$ . 238
- The locally heated surface of the sample ( $\Delta T \sim 500^\circ\text{C}$ ) (Ref. 26) does not 239
- have enough time to cool down before the next laser pulse arrives, further 240
- increasing the local temperature. 241
- <sup>26</sup>Y. Li, V. A. Stoica, L. Endicott, G. Wang, C. Uher, and R. Clarke, *Appl.* 242
- Phys. Lett.* **97**, 171908 (2010). 243
- <sup>27</sup>See supplementary material at <http://dx.doi.org/10.1063/1.3634014> for a 244
- detailed description of the experiment procedure, results and discussion. 245
- 246